ON THE HOMOGENEITY OF UNDISTURBED CLAY SAMPLES RETRIEVED FROM OSAKA BAY

Yoichi Watabe, Port and Airport Research Institute, Yokosuka, Japan
Tomoko Takemura, Port and Airport Research Institute, Yokosuka, Japan
Yasunori Shiraishi, Nippon Koei Co., Ltd., Tokyo, Japan
Tomohide Murakami, Saeki Kensetsu Kogyo Co., Ltd., Tokyo, Japan

ABSTRACT
Samples collected from both Holocene and Pleistocene layers in Osaka Bay were examined. The retrieved sample with a length of about 1 m was divided into every 25 mm in order to trim consolidation specimens, and the followings were examined: *i*) natural water content; *ii*) Atterberg's limits; *iii*) grain size fractions; *iv*) bulk density; *v*) particle density; *vi*) void ratio; *vii*) consolidation yield stress; *viii*) compression index; *ix*) coefficient of consolidation; and *x*) SEM photographing. The objective of this study is to evaluate variations of soil parameters obtained from laboratory tests. It is concluded that the variation of physical and mechanical properties is mainly influenced by macro-scale heterogeneity or sample disturbance, since specimen size for laboratory tests is sufficiently large on microscopic heterogeneity.

RÉSUMÉ
Les échantillons d'argile se sont rassemblés des couches holocène et pléistocène dans la baie d'Osaka ont été examinées. Les échantillons récupéré en une longueur d'environ 1 m a été divisé en tous les 25 millimètres afin d'couper des spécimens de consolidation, et les paramètres suivants ont été examinée: *i*) teneur en eau naturelle; *ii*) limites des liquidité et plasticité; *iii*) fractions de granulométrie; *iv*) densité en humide; *v*) densité des grains; *vi*) indice des vides; *vii*) pression de préconsolidation; *viii*) indice de compression; *ix*) coefficient de consolidation; et *x*) photographie de microscope électronique de balayage. L'objectif de cette étude est d'évaluer des variations des paramètres d'argile à la baie d'Osaka.

1. INTRODUCTION

Osaka Bay clay retrieved from the seabed was investigated for the Kansai International Airport project, which is constructed on an artificial island in Osaka Bay 5 km off the Senshu area 35 km southwest of Osaka City. The first phase of the Airport with only one runway was in operation from September, 1994, and the second phase is under construction for inauguration with two parallel runways in 2007. Consolidation parameters obtained from consolidation tests, carried out every 1—2 m depth(s), show a significant variation (Tanaka et al. 2003*a*). It has not been cleared yet whether the variation was caused by sample disturbance or derived from sample heterogeneity, even in a precise cone penetration test applied to great depths (Tanaka et al. 2003*b*).

In this study, samples collected from both Holocene and Pleistocene layers were examined. The retrieved sample with a length of about 1 m was divided into every 25 mm in order to trim consolidation specimens, and the following parameters were examined: *i*) natural water content (w_n); *ii*) Atterberg's limits (w_L and w_p); *iii*) grain size fractions (clay fraction, silt fraction, and sand fraction); *iv*) bulk density (ρ_t); *v*) particle density (ρ_s); *vi*) void ratio (*e*); *vii*) consolidation yield stress (p'_c); *viii*) compression index (C_c); *ix*) coefficient of consolidation (c_v); and *x*) scanning electron microscopic (SEM) photographing. The objective of this study is to evaluate variations of soil parameters obtained from laboratory tests. The test program corresponding to the divided samples is listed in Table 1.

Table 1. List of tested samples.

Elevation EL. (–m)	Atter-berg limits	Grain size	CRS	SEM	Elevation EL. (–m)	Atter-berg limits	Grain size	CRS	SEM
37.500–37.525		○	○		125.500–125.525				
37.525–37.550	○	○	○	○	125.525–125.550	○	○		○
37.550–37.575		○	○		125.550–125.575				
37.575–37.600		○	○		125.575–125.600			○	
37.600–37.625			○		125.600–125.625			○	
37.625–37.650	○	○	○	○	125.625–125.650	○	○		○
37.650–37.675		○	○		125.650–125.675			○	
37.675–37.700		○	○		125.675–125.700			○	
37.700–37.725		○	○		125.700–125.725				
37.725–37.750		○	○		125.725–125.750			○	
37.750–37.775	○	○	○		125.750–125.775	○	○		○
37.775–37.800		○	○	○	125.775–125.800			○	
37.800–37.825		○	○		125.800–125.825			○	○
37.825–37.850	○	○	○		125.825–125.850	○	○	○	
37.850–37.875		○	○	○	125.850–125.875			○	
37.875–37.900		○	○		125.875–125.900			○	
37.900–37.925		○	○		125.900–125.925		○	○	
37.925–37.950	○	○	○		125.925–125.950	○	○	○	○
37.950–37.975		○	○	○	125.950–125.975		○	○	
37.975–38.000		○	○		125.975–126.000		○	○	
38.000–38.025		○	○	○	126.000–126.025		○	○	○
38.025–38.050	○	○	○		126.025–126.050	○			
38.050–38.075		○	○		126.050–126.075		○	○	
38.075–38.100		○	○		126.075–126.100		○	○	
38.100–38.125		○	○	○	126.100–126.125		○	○	
38.125–38.150	○	○	○		126.125–126.150	○	○	○	
38.150–38.175		○	○		126.150–126.175		○	○	○
38.175–38.200		○	○	○	126.175–126.200		○	○	
38.200–38.225		○	○	○	126.200–126.225		○	○	
38.225–38.250	○	○	○	○	126.225–126.250	○	○	○	
38.250–38.275		○	○		126.250–126.275		○	○	○
38.275–38.300		○	○		126.275–126.300		○	○	
38.300–38.325					126.300–126.325				
38.325–38.350					126.325–126.350	○			
38.350–38.375					126.350–126.375				
38.375–38.400					126.375–126.400				
38.400–38.425					126.400–126.425				
38.425–38.450					126.425–126.450	○			
38.450–38.475					126.450–126.475				
38.475–38.500					126.475–126.500				

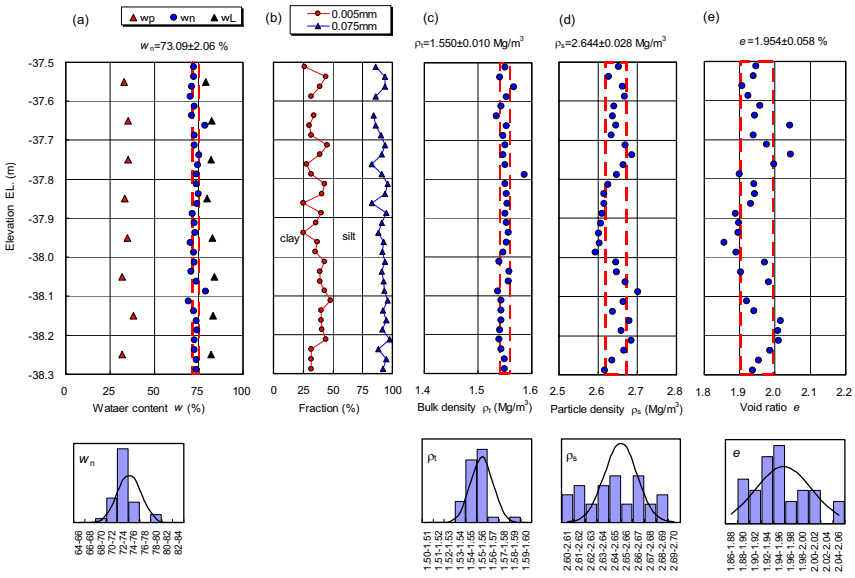

Figure 1. Profiles of physical properties with depth in the Holocene clay.

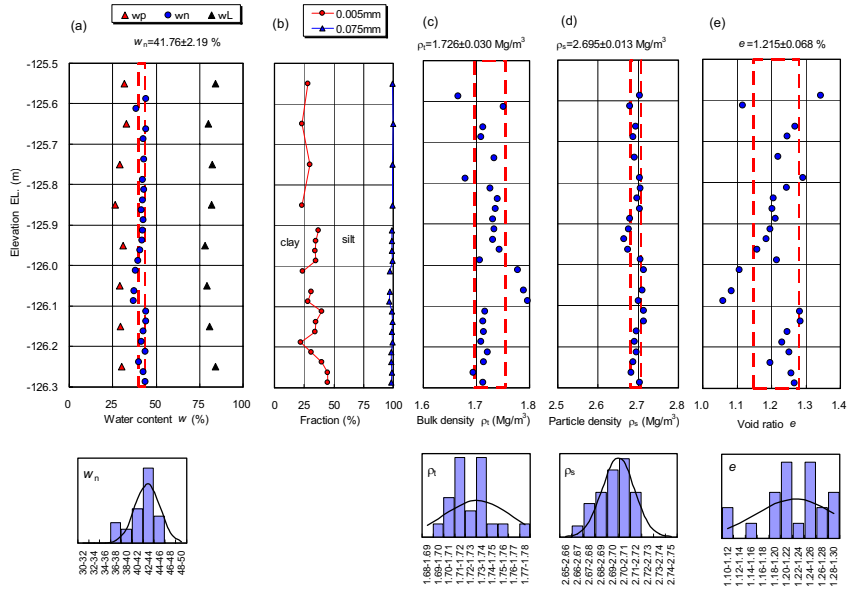

Figure 2. Profiles of physical properties with depth in the Pleistocene clay.

2. SAMPLE

Osaka Bay clay examined in this study was sampled during the ground survey for the second phase construction of Kansai International Airport. The deep sampling was effectively carried out by PARI (formerly PHRI) wire line method (Horie et al. 1984; Kanda et al. 1991) as illustrated in Watabe et al. 2002. At the sampling site, the water depth was 19 m, the thickness of Holocene clay layer was 25 m, and the Pleistocene clay deposited more than 350 m thick alternately with some sandy layers. The clay at G.L. –120 deposited 270,000 years ago. The clay layer shows slight overconsolidation (OCR = 1.1—1.5), but it is, generally, in normal consolidation (Akai et al. 1995; Akai, 2000; Watabe et al. 2002). Tanaka and Locat (1999) indicated that the consolidation behavior is possibly characterized by the diatoms which are abundantly contained in the Osaka Bay clay. In this study, both samples retrieved from a Holocene

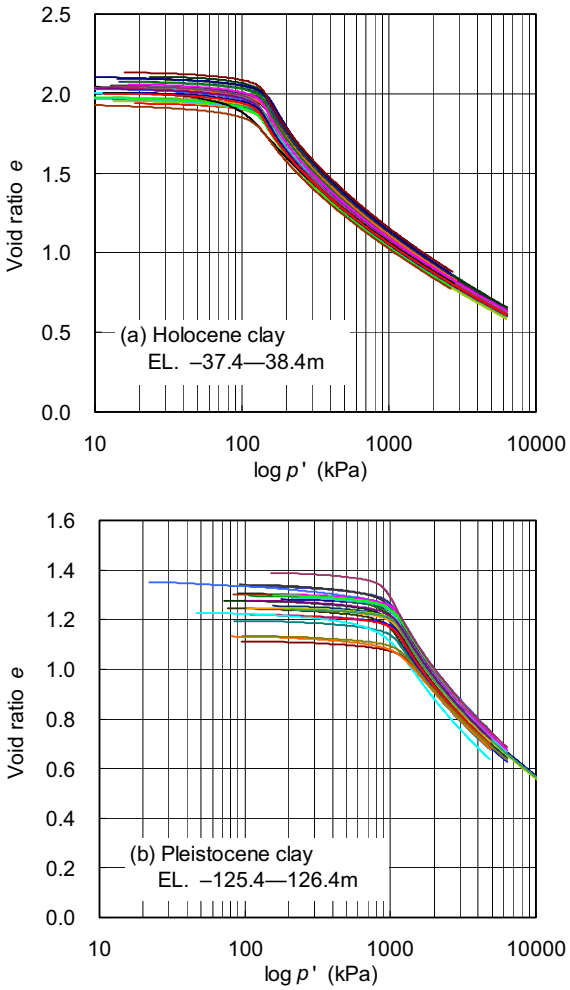

Figure 3. Relationships between void ratio and consolidation pressure.

layer (EL.–126 / G.L.–107 m) and a Pleistocene layer (EL. –38 / G.L. –19 m) were examined.

3. TEST PROGRAM

Atterberg's limits (w_L and w_p), soil particle density (ρ_s), and grain size distribution were examined before carrying out the series of consolidation tests; then the constant rate strain consolidation tests (CRS tests) were carried out. Natural water content (w_n), bulk density (ρ_t), void ratio (e), consolidation yield stress (p'_c), compression index (C_c), compression index at a consolidation pressure of greater than 5,000 kPa (C_c*), and coefficient of consolidation (c_v) were obtained from the CRS tests. The specimens, trimmed into a size of 60 mm in diameter and 20 mm in height, were examined with a back pressure of 98.1 kPa and in a strain rate of 0.02%/min.

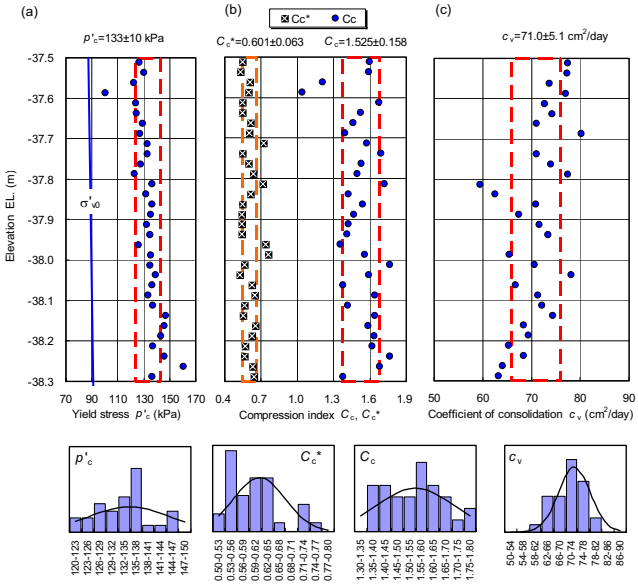

Figure 4. Profiles of consolidation properties with depth in the Holocene clay.

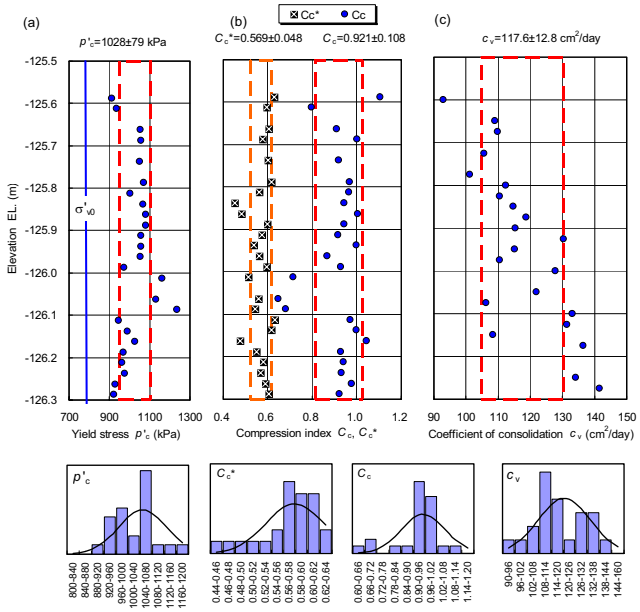

Figure 5. Profiles of consolidation properties with depth in the Pleistocene clay.

Using soil chips from specimen trimming, microfabric was SEM-photographed. In the specimen preparation for SEM, freeze-cut-drying method (Kang et al. 2003) was adopted to minimize the sample disturbance and to obtain a flat observation surface. Four positions every 0.3 mm on each specimen were photographed by 4 different magnifications

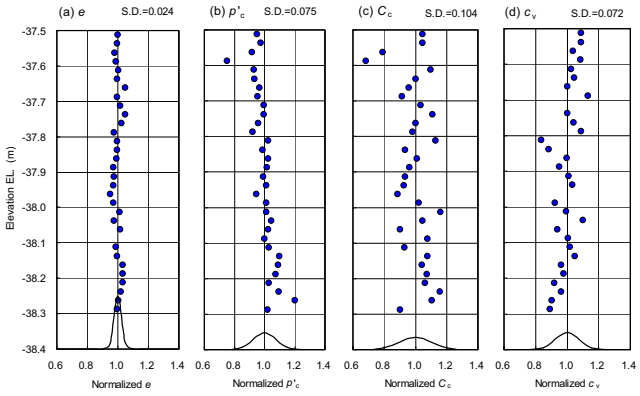

Figure 6. Profiles of normalized consolidation parameters with depth in the Holocene clay.

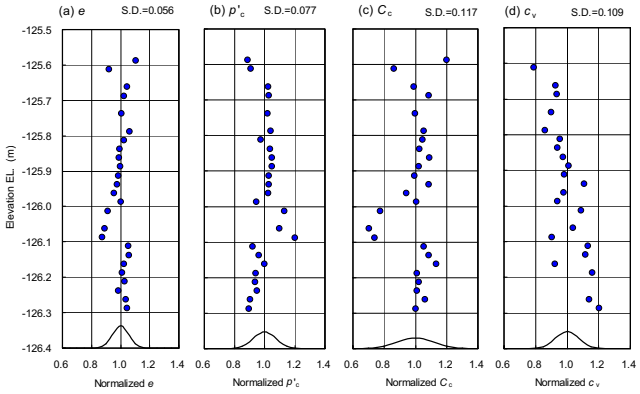

Figure 7. Profiles of normalized consolidation parameters with depth in the Pleistocene clay.

as 5000, 2500, 1000, and 500 times. The SEM photographs were image-analyzed by using the free-software "Scion Image", which can transform the photographed image in gray scale (0—256) into a binarized image with a threshold value. In this study, a threshold value of 200 was adopted. The black percentage in the binarized black and white image was calculated.

4. TEST RESULTS

4.1 Physical and consolidation properties

Physical properties of the Holocene and the Pleistocene clays are shown in Figures 1 and 2, respectively. Frequencies of w_n, ρ_t, ρ_s, and e, the mean value (MV), and the standard deviation (SD) are also shown in the figures. Both clays have essentially common properties as w_L = 80%, w_p = 30%, plasticity index (I_p) of 50, clay fraction (<5 μm) of 30—40%, sand fraction (>75 and <2 μm) of 0—20%. The w_n of the Holocene clay (73.09±2.06%) is slightly less than w_L, and w_n of the Pleistocene clay (41.76±2.19%) is slightly larger than w_p. For the both clays, SD of w_n is only about 2%. The profile of ρ_t of the Holocene clay (1.550±0.010 Mg/m^3) is very homogeneous; however, that of the Pleistocene clay (1.726±0.030 Mg/m^3) shows slightly larger variation caused by a high ρ_t value close to 1.8 Mg/m^3 at around EL. –126.05 m (w_n shows a slightly smaller value).

The profile of ρ_s of the Holocene clay (=2.644±0.028 Mg/m^3) is slightly variable, corresponding to the profile of e (1.954±0.058). The ρ_s shows high values of 2.69—2.70 Mg/m^3 at round EL. –37.75 m and –38.15 m resulting higher e values. This fact means that, if MV of 2.644 Mg/m^3 was adopted as ρ_s to calculate e for all depths, e could show a very homogeneous profile. It cannot be judged between the profile of ρ_s and the constant value of ρ_s. On the other hand, the profile of ρ_s of the Pleistocene clay (=2.695±0.013 Mg/m^3) is very homogeneous. Thus, the profile of e corresponds to the profile of ρ_t. The profiles at EL. –125.05 m indicate that this depth is silty; however, this cannot be clearly confirmed from grain size fractions and SEM images (Figure 11).

Relationships between void ratio and consolidation stress (e–log p') for (a) Holocene clay and (b) Pleistocene clay are shown in Figure 3. All curves for both clays converge a curve under high p', though initial e values show some variation. The inversed S-shaped curves, even Holocene clay, are characteristically observed as aged clay. The curve without a clear yielding point in Figure 3*a* is EL. –37.59 m, and the three curves from smaller e values in Figure 3*b* are around EL. –126.05 m.

Profiles of p'_c, C_c, C_c*, and c_v with depth for the Holocene and the Pleistocene clays are shown in Figures 4 and 5, respectively.

In the Holocene clay, p'_c (=133±10 kPa) slightly increases with depth. The SD of C_c is 0.158, but the SD of C_c* is only 0.063. However coefficient of variation (CV) defined by the ratio of SD to MV (CV=SD/MV) is the same as 10% for both C_c and C_c*. In addition, the specimen from EL. –37.59 m, which shows smaller p'_c and C_c possibly caused by sample disturbance, is not identified in the profile of C_c*.

In the Pleistocene clay, p'_c is evaluated as 1028±79 kPa, but it shows a larger p'_c at around EL. –126.05 m. This larger p'_c is caused from the unclear p'_c on the sloping shoulder of e–log p' curves as shown in Figure 3*b*. C_c=0.921±0.108 and C_c*=0.569±0.048 are about 60% and 95% of those in the Holocene clay, respectively, indicating that both clays are essentially the same consolidation properties in normal consolidation range. The C_c/C_c* is calculated as 1.6, which is smaller than that of 2.5 calculated in the Holocene clay.

In order to evaluate the variation of e, p'_c, C_c, and c_v, these parameters are normalized by their mean values, respectively, and profiles of the normalized parameters of the Holocene and Pleistocene clays with depth are shown in Figures 6 and 7, respectively.

In the Holocene clay, SD values of normalized e, p'_c, C_c, and c_v are 0.024, 0.075, 0.104, and 0.072, respectively. SD

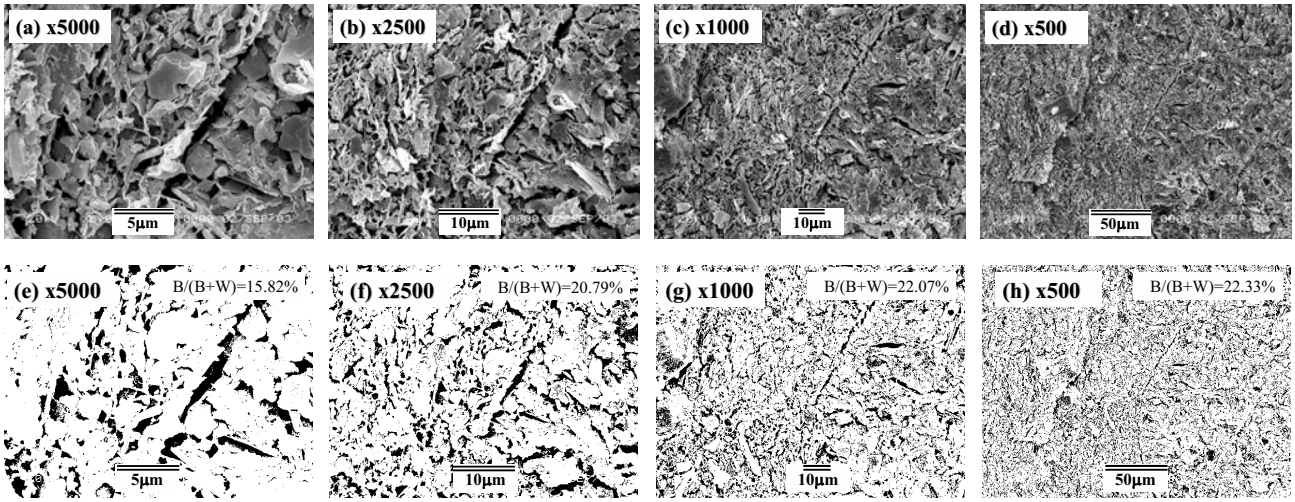

Figure 8. SEM and binarized images of the Holocene clay at EL. –37.96 m.

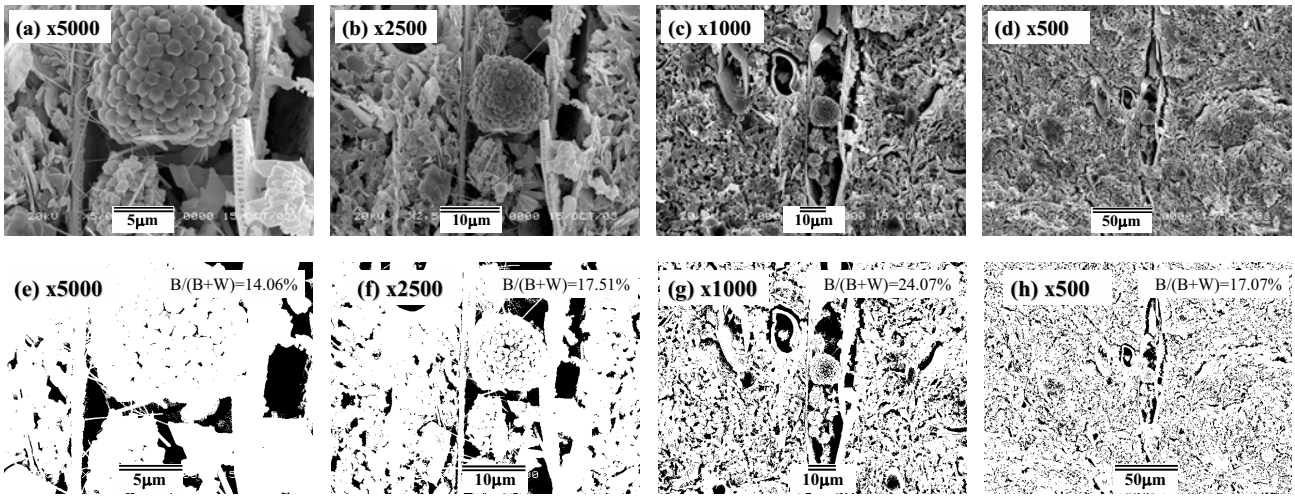

Figure 9. SEM and binarized images of the Holocene clay at EL. –38.19 m.

of e is the smallest and that of C_c is the largest among them. In the Pleistocene clay, SD of normalized e of 0.056 is about twice of that in the Holocene clay, caused from the smaller e values at around EL. –126.05 m. SD of normalized p'_c is 0.077, which is almost the same as that in the Holocene clay. SD of normalized C_c of 0.117 is also the same level as that in the Holocene clay. However, SD of normalized c_v of 0.109 is 50% larger than that in the Holocene clay.

Examining the clay samples, divided into every 25 mm, retrieved from both Holocene and Pleistocene layers in Osaka Bay resulted that the clay layers are relatively homogeneous with SD values of the normalized parameters (e, p'_c, C_c, and c_v) in a range of 2.5—12.0%. SD of normalized e is only 2.5% in the Holocene clay and 5.6% in the Pleistocene clay, but SD values of the consolidation parameters (p'_c, C_c, and c_v) obtained from CRS tests are greater than these. Since, in an ordinary ground survey for design, consolidation parameters are examined every one or a few meter(s), it is difficult to evaluate the variation of obtained parameters; thus, it cannot be determined if the tested specimen was representative of the examining layer. Accordingly, it is important to select representative specimens in the layer considering the profiles of physical properties.

4.2 SEM observation

Observed SEM images and those binarized images for the Holocene clay at EL. –37.96 and –38.19 m and the Pleistocene clay at EL. –125.54 and –126.01 m are shown in Figures 8, 9, 10, and 11, respectively. In Figures 8 and 11,

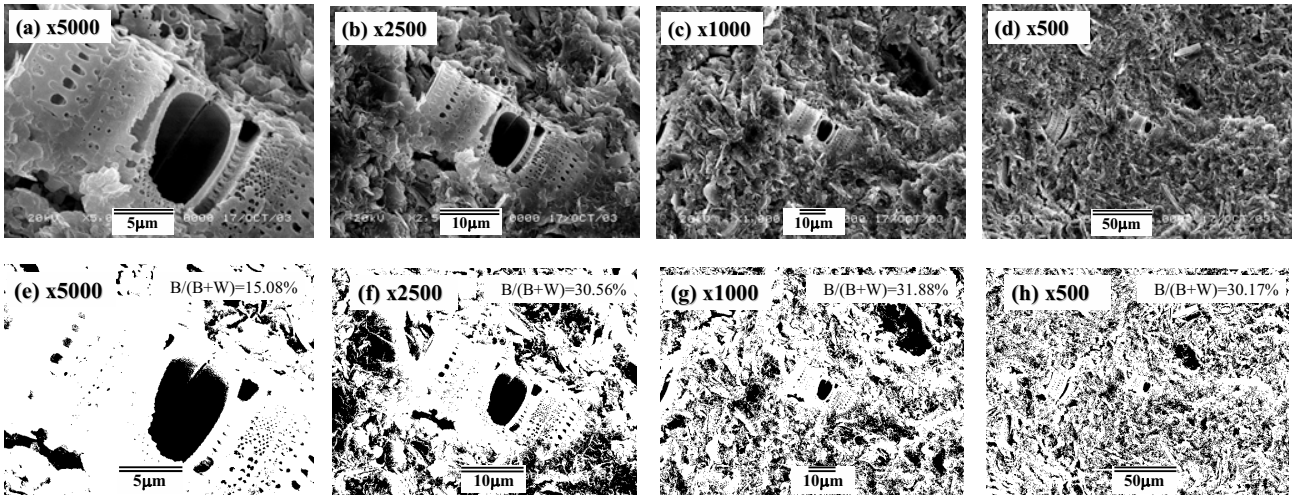

Figure 10. SEM and binarized images of the Pleistocene clay at EL. –125.54 m.

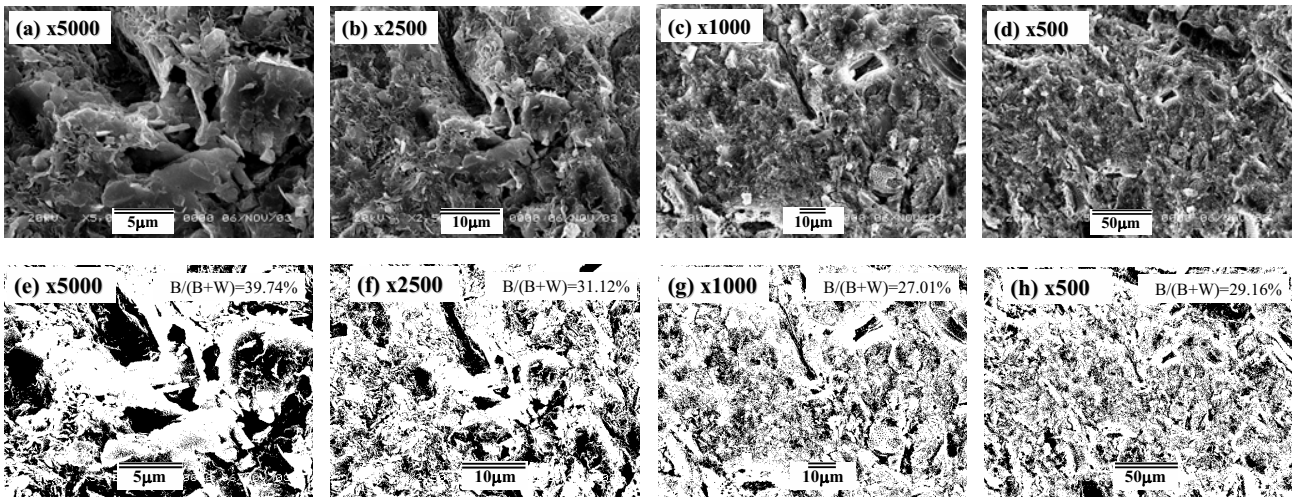

Figure 11. SEM and binarized images of the Pleistocene clay at EL. –126.01 m.

the images in magnification of both 5000 and 2500 times show enlarged structure of soil fabric. On the other hand, in Figures 9 and 10, the images in magnification of both 5000 and 2500 times show particular parts on pyrite (Figure 9) and diatom (Figure 10), not representing the soil fabric.

Profiles with depth (a—d) and frequencies (e—h) on black percentage in the binarized black and white images for the Holocene and the Pleistocene clays are shown in Figures 12 and 13, respectively. Width shown by broken line shows a range of MV±SD. The width tends to decrease when the magnification decreases.

In the Holocene clay (Figure 12), SD decreases when the magnification decreases as 5000, 2500, and 1000 times, indicating that the impression of the SEM images could change. However, SD values of both magnifications of 1000 and 500 times are at the same level. This fact can be visually impressive in Figure 8.

In the Pleistocene clay (Figure 13), SD tends to decrease when the magnification decreases. SD of the magnification of 2500 times is about half of that of 5000 times, but SD values of 2500, 1000, and 500 times are at the same level of around 6%. This fact can be visually impressive in Figure 11.

In the Holocene clay, SD values of the magnification of 2500 times and both 1000 and 500 times are 72% and 48%, respectively, of that of 5000 times. This indicates that every SEM image with a high magnification gives different impression, but that with a low magnification of either 1000

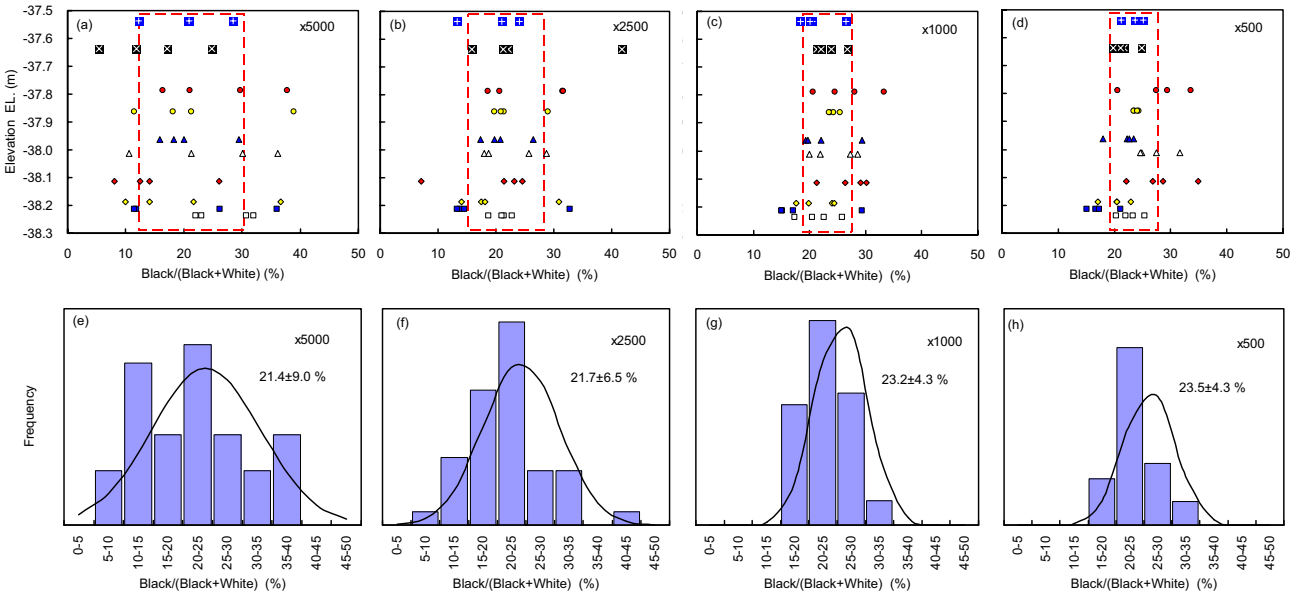

Figure 12. Profiles of black percentage with depth and frequencies of the binarized images in the Holocene clay.

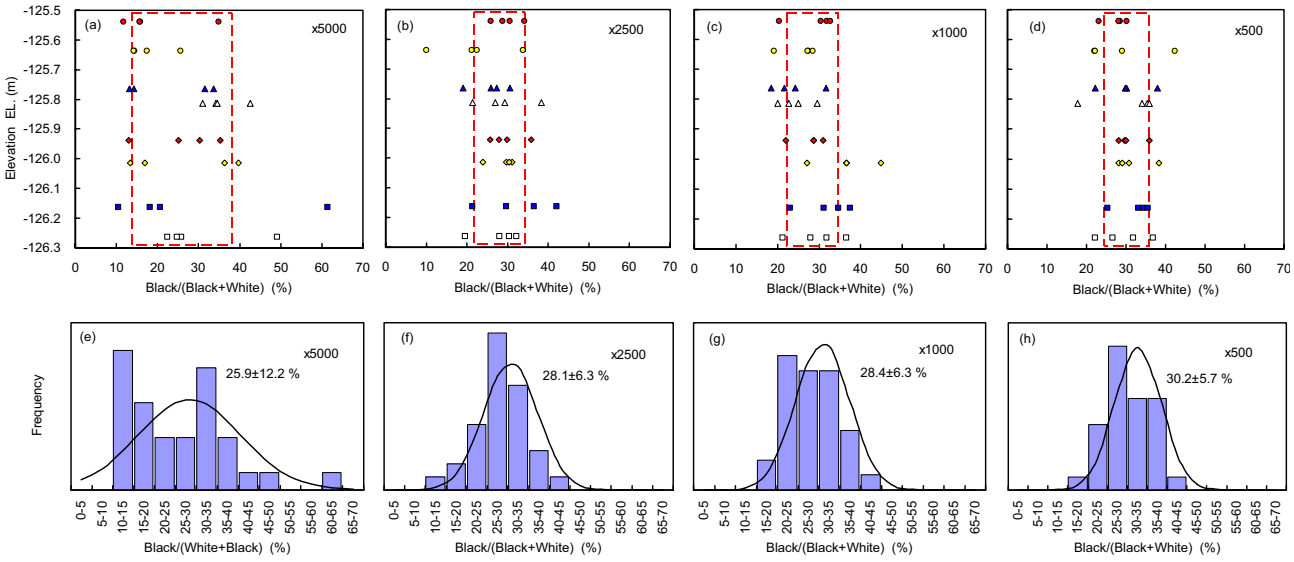

Figure 13. Profiles of black percentage with depth and frequencies of the binarized images in the Pleistocene clay..

or 500 times gives the similar impression. In the Pleistocene clay, SD value of the magnification of 2500 times is 52% of that of 5000 times, and that of either 2500, 1000, or 500 times is at the same level.

Figure 14 shows relationships (a) MV of black percentage and (b) CV of black percentage versus the magnification. In Figure 14*a*, MV slightly decreases when the magnification increases, but essentially constant. From CV in Figure 14*b*, it can be said that the variation of the SEM images becomes significant when observation magnification is greater than 1000 and 2500 times for the Holocene and Pleistocene clays, respectively. Therefore, a representative structure in the microfabric could be observed in an area of 150×120 μm with the magnification of 1000 times for the Holocene clay and 50×40 μm with the magnification of 2500 times for the Pleistocene clay. Since specimen size for laboratory tests is sufficiently large on microscopic heterogeneity, the variation

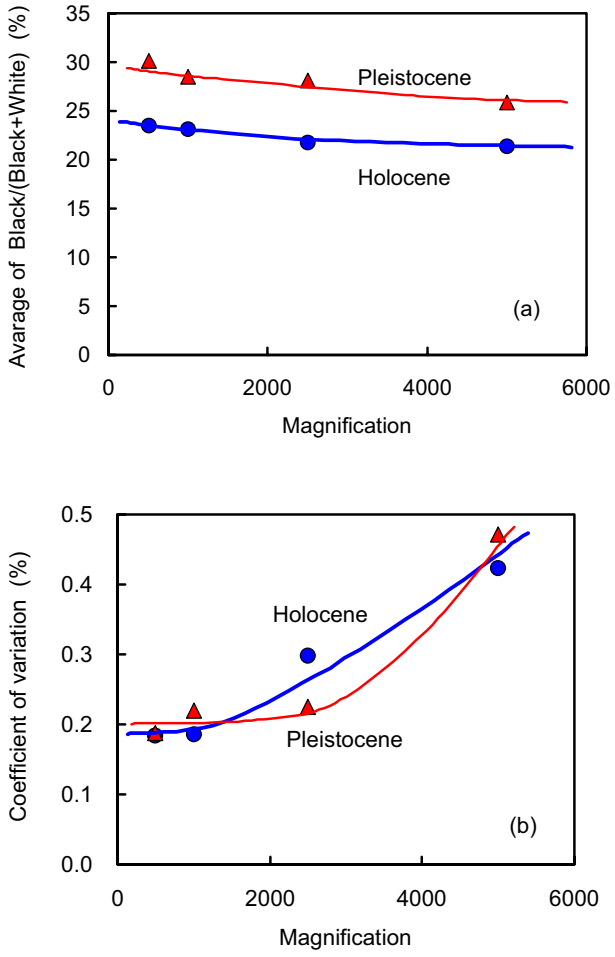

Figure 14. Relationships of (a) average of black percentage and (b) coefficient of variation versus the observation magnification.

h retrieved from either Holocene or Pleistocene layer in Osaka Bay was divided into every 25 mm in order to exam the variation of both physical and consolidation properties. The followings are derived as conclusions: the clay layers are relatively homogeneous with SD values of the normalized parameters (e, p'_c, C_c, and c_v) in a range of 2.5—12.0%. SD of normalized e is only 2.5% in the Holocene clay and 5.6% in the Pleistocene clay, but SD values of consolidation parameters (p'_c, C_c, and c_v) obtained from CRS tests are greater than these. It can be said that the variation of the SEM images becomes significant when observation magnification is greater than 1000 and 2500 times for the Holocene and Pleistocene clays, respectively. Since specimen size for laboratory tests is sufficiently large on microscopic heterogeneity, the variation of physical and mechanical properties is mainly influenced by macro-scale heterogeneity or sample disturbance.

of physical and mechanical properties is mainly influenced by macro-scale heterogeneity or sample disturbance.

5. CONCLUSIONS

In this study, clay sample in 1 m length eac

REFERENCES

Akai, K. 2000. Insidious settlement of super-reclaimed offshore seabed, Coastal Geotechnical Engineering in Practice, Balkema, pp. 243-248.

Akai, K., Nakaseko, K., Matsui, T., Kamon, M, Sugano, K., Tanaka, Y., and Suwa, S. 1995. Geotechnical and geological studies on seabed in Osaka Bay, Proceedings of the 11th European Conference on Soil Mechanics and Foundation Engineering, Vol. 8, pp. 1-6.

Horie, H., Zen, K., Ishii, I., and Matsumoto, K. 1984. Engineering properties of marine clay in Osaka Bay, (Part-1) Boring and sampling, Technical Note of the Port and Harbour Research Institute, Ministry of Transport, Japan, No. 498, 5-45. (in Japanese)

Kanda, K., Suzuki, S., and Yamagata, N. 1991. Offshore soil investigation at the Kansai International Airport, Proceedings of the International Conference on Geotechnical Engineering for Coastal Development, Geo-Coast '91, Vol. 1, pp. 33-38.

Kang, M.-S., Watabe, Y., and Tsuchida, T. 2003. Effect of drying process on the evaluation of microstructure of clays using scanning electron microscope (SEM) and mercury intrusion porosimetry (MIP), Proceedings of the 13th International Offshore and Polar Engineering Conference, pp. 385-392.

Tanaka, H. and Locat, J. 1999. A microstructural investigation of Osaka Bay clay: the impact of microfossils on its mechanical behaviour, Canadian Geotechnical Journal, Vol. 36, pp. 493-508.

Tanaka, H., Ritoh, F., and Omukai, N. 2003*a*. Geotechnical properties of clay deposits of the Osaka Basin, Characterisation and Engineering Properties of Natural Soils, Swets & Zeitlinger, pp. 455-474.

Tanaka, H., Tanaka, M., Suzuki, S., and Sakagami, T. 2003*b*. Development of a new cone penetrometer and its application to great depths of Pleistocene clays, Soils and Foundations, Vol. 43, No. 6, pp. 51-61.

Watabe, Y., Tsuchida, T., and Adachi, K. 2002. Undrained shear strength of Pleistocene clay in Osaka Bay, Journal of Geotechnical and Geoenvironmental Engineering, ASCE, Vol. 128, pp. 216-226.